Experimental investigation of the effect of bypass inlet on flow boiling in a mini/micro-channel

Raamkumar Loganathan, Ahmed Mohiuddin, Sateesh Gedupudi*

Heat Transfer and Thermal Power Laboratory, Department of Mechanical Engineering, Indian Institute of Technology Madras, Chennai, India

ARTICLE INFO

ABSTRACT

The present work reports the findings from an experimental study on the effect of bypass inlet on the performance of flow boiling of water in a copper mini/micro-channel of dimension 2.5 mm wide x 0.6 mm deep x 25 mm long. The mass fluxes considered were 430 kg/m^2 s, 640 kg/m^2 s and 850 kg/m^2 s and the heat flux was in the range 87–548 kW/m^2. The results show a significant increase in heat transfer coefficient with the increase in bypass ratio for the subcooled boiling conditions and the enhancement decreases with the increase in the exit quality. An increase in pressure drop was also noticed due to the bypass inlet. The study indicates potential for further investigation and optimization.

1. Introduction

It is well known that there is currently an increasing demand for better cooling techniques to remove high heat fluxes associated with the rapid miniaturization of electronic systems. Higher heat flux removal capacity of micro-channel heat sinks was first demonstrated in 1981 by Tuckerman and Pease [1]. Critical heat flux limits and flow instabilities are the primary challenges being faced in implementing the two-phase micro-channel heat sinks in practical applications. Many techniques have been studied and proposed to increase the critical heat flux limits and to reduce instabilities caused by various sources [2–8]. While there is considerable research being carried out in the direction of understanding the physical mechanisms and instabilities involved in two-phase micro-channel heat sinks, there is also a need to develop techniques to enhance its heat transfer performance [9,10]. As reviewed by Kandlikar et al. [2], Sidik et al. [11], Narendran et al. [12] and Lu and Vafai [13], a number of different methods like introducing micro-fins, oblique fins, staggered fins, nanostructures, ribs and cavities, dimples and grooves, double-layered/stacked micro-channels, interconnected micro-channels, wavy micro-channels, bi-furcated micro-channels, branching and fractal micro-channels have been investigated and proposed to enhance the heat transfer in micro-channels. Nearly all of these methods augmented heat transfer coefficients by flow disruption through geometrical modifications and a majority of them are implemented for single phase flows [14,15]. Most of the flow boiling enhancement techniques in micro-channels involved surface modifications [16,17] and use of nano-fluids [18,19]. Recently,

researchers started focusing on the enhancement of flow boiling performance through geometrical optimization like expanding channels [20,21], tapered manifolds [22], straight and oblique-finned micro-channels [23–25], stepped-fin micro-channels [26].

Hybrid cooling schemes involving micro-channel flows and jet impingement have proved to be an effective way to achieve higher cooling fluxes and uniform temperatures that are unattainable with individual cooling schemes [27,28]. The hybrid cooling scheme implemented by Sung and Mudawar [29] involved impingement of circular jets with micro-channel flow [30]. The working fluid entered into each micro-channel as a series of jets and exited symmetrically through the outlets (on either side) of the channel. This scheme was able to remove high heat flux without encountering critical heat flux. The scheme was tested with both single and two-phase flows. They noticed a different two phase behavior, i.e., the observed bubble nucleation, growth, departure and coalescence were different from those commonly observed in conventional micro-channels. The subcooled jets were found to break the bubbles repeatedly unlike the uninterrupted bubble growth in conventional micro-channels.

Similar hybrid scheme which combined the benefits of micro-channel flow and jet impingement was also investigated by Barrau et al. [31,32] for single phase flow. Their work also showed that the hybrid scheme resulted in improved uniformity in the surface temperature of the cooled object. They concluded that the desired surface temperature profiles can be achieved on the cooled object by varying the internal geometry of the hybrid scheme. This work was also tested experimentally under real outdoor conditions for a densely packed photovoltaic cells [33].

---

* Corresponding author at: Department of Mechanical Engineering, Indian Institute of Technology Madras, Chennai 600 036, India.
E-mail address: sateeshg@iitm.ac.in (S. Gedupudi).

From the review of literature, it can be seen that the full potential of two-phase micro-channel heat sinks is still unexplored and there is a need for newer and better techniques. It can be concluded that the combination of micro-channel flow and jet impingement can be one of the methods to maximize the benefits of two-phase micro-channel heat sinks. However, there are complexities involved in implementing both the techniques together and there is also difficulty in removing the spent coolant effectively. Hence, more research is needed in this direction.

1.1. Objective of the current work

In the present study, to overcome the difficulty associated with the combined micro-channel flow and jet impingement, a secondary or bypass inlet is introduced halfway between the channel primary inlet and the channel outlet, such that the flow in the channel takes place in only one direction. DI water enters the channel through both primary inlet and bypass inlet and exits through a single outlet. Even though the proposed technique doesn't involve exactly the jet impingement process, the flow closely resembles the jet action. The current experimental study investigates the effect of the proposed bypass inlet on the flow boiling heat transfer characteristics of a mini/micro-channel.

1.2. Proposed scheme

The proposed scheme is shown in Fig. 1. The design consists of two passages, a primary passage and a secondary passage. Both the passages are parallel and secondary passage lies atop the primary passage. Width and depth of the secondary passage are the same as those of primary. Bypass inlet to the micro-channel is a 90° vertical hole. It connects both the passages exactly at the middle of the primary passage. Further details of the proposed scheme are described in Section 2.2.

2. Experimental setup

2.1. Experimental circuit

The closed loop experimental circuit consists of a reservoir, sub-cooler, micro-gear pump, preheaters, test section, condenser, chiller unit, data acquisition system and control panel. A schematic of the experimental circuit is shown in Fig. 2(a) and a photograph of the experimental setup is shown in Fig. 2(b). De-ionized (DI) water was used as the working fluid for all the experiments. The reservoir was fitted with a cartridge heater and a reflux condenser for high temperature degasification. A sub-cooler brings down the temperature of DI water below 30 °C before it enters the micro-gear pump (Ismatec Reglo-Z). Two Swagelok micro-filters were installed along the circuit – one of mesh size 90 μm before the gear pump and the other of mesh size 0.5 μm before the test section. Two different preheaters were employed to preheat the DI water entering the primary and secondary passages separately. While the total flow rate was measured by Emerson Coriolis mass flow meter (CMFS010M), flow rate into primary passage was measured by a rotameter. The flow rate into the secondary passage is then the difference between the total and the primary flow rates. Water temperature at the outlet of both preheaters and water temperature inside the reservoir were maintained using PID controlled

cartridge heaters. The two-phase mixture leaving the test section was condensed in a counter-flow condenser. A common chiller unit was employed to cool the hot water coming from the condenser, the sub-cooler and the reflux condenser. Channel inlet pressure and differential pressure between the channel inlet and outlet were measured by Yokogawa EJA110E diaphragm type pressure transmitters. A Honeywell miniature pressure sensor (26PCCFA6G) was used at the entry of working fluid into the secondary passage. Pressures and temperatures were measured at different locations in the circuit using pressure gauges and stainless steel shielded K-type thermocouples, respectively. Flow rate, channel pressure and temperature data were acquired with the aid of LabVIEW software using National Instruments data acquisition system.

2.2. Test section

Primary passage is the conventional micro-channel. In contrast to sending the total mass flow through a single passage as in the conventional micro-channel, a fraction of the working fluid is sent through the primary inlet. The remaining is sent through the secondary passage to the bypass inlet located at the middle of the channel. The secondary passage does not participate in the heat transfer process.

Figs. 3(a) and 3(b) present the sectional view and the exploded view of the test section, respectively. Pictures of different components of the test section are presented in Fig. 4. A 2.5 mm wide, 0.6 mm deep and 25 mm long micro-channel was machined in an oxygen-free copper block. Inlet and outlet plenums of the channel were made of Teflon and inserted into the copper block as shown in Fig. 4(a) to avoid any heat transfer at the plenums. Five holes of 1 mm diameter, three on one side and two on the other side, were drilled in copper to insert K-type thermocouples which were used to obtain channel wall temperatures. Thermocouples were placed 3 mm below the micro-channel bottom wall. A cartridge heater placed parallel to micro-channel at the bottom of the copper block was used as the heat source. Insulation around the copper block was provided by a surrounding Teflon block. Top cover of the test section was made of transparent polycarbonate (Lexan) which included the inlet and outlet passages of the micro-channel.

Detail A of Fig. 3(a) shows the primary and secondary passages connected by the bypass inlet. Primary passage and secondary passage were machined in copper and Lexan polycarbonate, respectively. A 1 mm thick transparent polycarbonate mid-plate was placed in between copper and top polycarbonate cover. A hole of 2 mm diameter drilled in polycarbonate mid-plate acted as the bypass inlet. Mid-plate also includes two more holes which connect the inlet and outlet Teflon plenums of micro-channel with the inlet and outlet of test section, respectively. Viton rubber O-rings were used to prevent any possible leakage by providing proper sealing. One O-ring was placed around the primary passage between copper block and polycarbonate mid-plate and another around the secondary passage between polycarbonate mid-plate and polycarbonate top cover. The average surface roughness of micro-channel was measured to be 1.36 μm.

2.3. Experimental procedure

All inlets and outlets in the reservoir were closed initially except the top vent to atmosphere (located on top of the reflux condenser) which
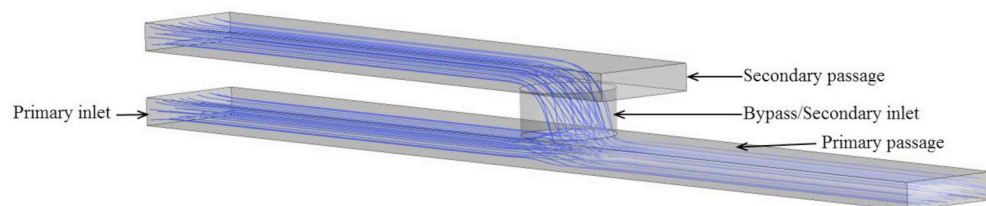

Fig. 1. Sketch of hybrid micro-channel geometry used in the present work.

Secondary passage

Primary inlet

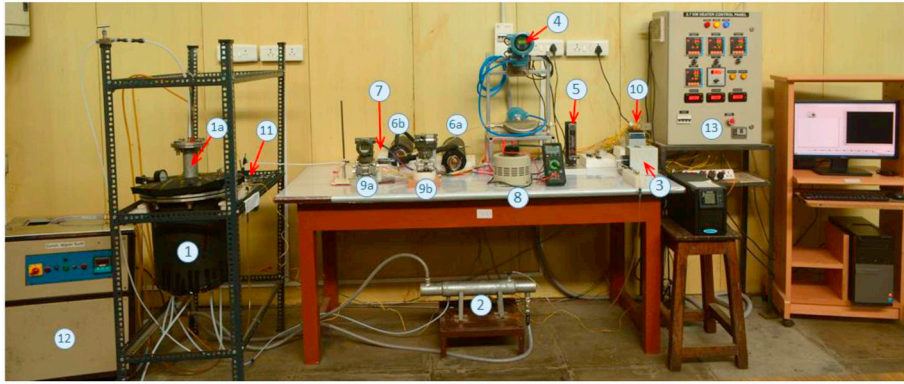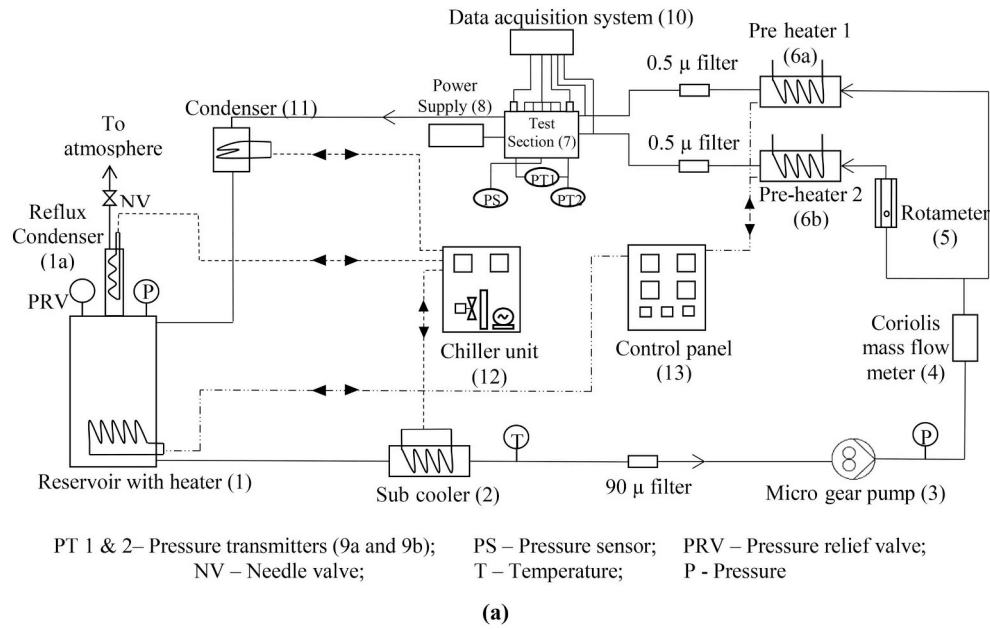Bypass/Secondary inlet

Primary passage

Fig. 2. The experimental setup: (a) schematic and (b) photograph.

was kept open partly using a needle valve. DI water in the reservoir was degassed by heating to a temperature above 100 °C using cartridge heater until pressure indicated by the reservoir pressure gauge reached the saturated pressure corresponding to the reservoir temperature. During this heating process, the dissolved gases in DI water escaped through the vent and water vapor condensed into water when it came in contact with the surface of reflux condenser. Reservoir was maintained at this state for 30 min. Above degasification procedure was repeated for another 30 min with the reservoir outlet and inlet open and DI water pumped through the experimental circuit. It was ensured that the reservoir pressure eventually reached the saturation pressure corresponding to the tank fluid temperature and then was maintained at this pressure, which indicated the negligible concentration of dissolved gases. The pressure inside the reservoir was always kept slightly higher than the atmospheric pressure to eliminate the possibility of air leaking into the reservoir.

Mass flow rate through the test section was varied using the Micro Gear Pump operating panel. Outlet temperatures of both the preheaters were maintained at 97 °C. Heat was supplied to the test section by setting the required voltage to the cartridge heater. Mass flow, pressure and temperature readings were monitored through LabVIEW and readings were recorded when all of them reached steady values. The same procedure was repeated for different heat flux values. Experiments were conducted for: (a) 430 kg/m² s with 50% bypass

ratio, (b) 640 kg/m² s with 33%, 50% and 66% bypass ratios, (c) 850 kg/m² s with 25%, 50% and 75% bypass ratios. Without bypass, i.e., with the entire flow delivered to the primary inlet of the channel, experiments were conducted for the same total mass fluxes. Bypass ratio is defined as the ratio of the flow rate through the secondary passage (bypass inlet) to the total flow rate through the primary and bypass inlets.

3. Data reduction

Total heat supplied to the heat sink and the heat removed by the fluid flow through the micro-channel in single-phase flow experiments are given by the Eqs. (1) and (2), respectively.

$$Q_{supplied} = VI \tag{1}$$

$$Q = \dot{m}c_p(T_o - T_i) \tag{2}$$

Heat loss from the test section is determined using Eq. (3)

$$Q_{loss} = VI - \dot{m}c_p(T_o - T_i) \tag{3}$$

However, for flow boiling experiments, it is not possible to obtain the heat loss values directly as above. Heat loss from the test section is characterized by obtaining a correlation between Q_{loss} and $(\overline{T}_{tc} - T_{atm})$ from single-phase experiments. Fig. 5 presents the plot between Q_{loss}
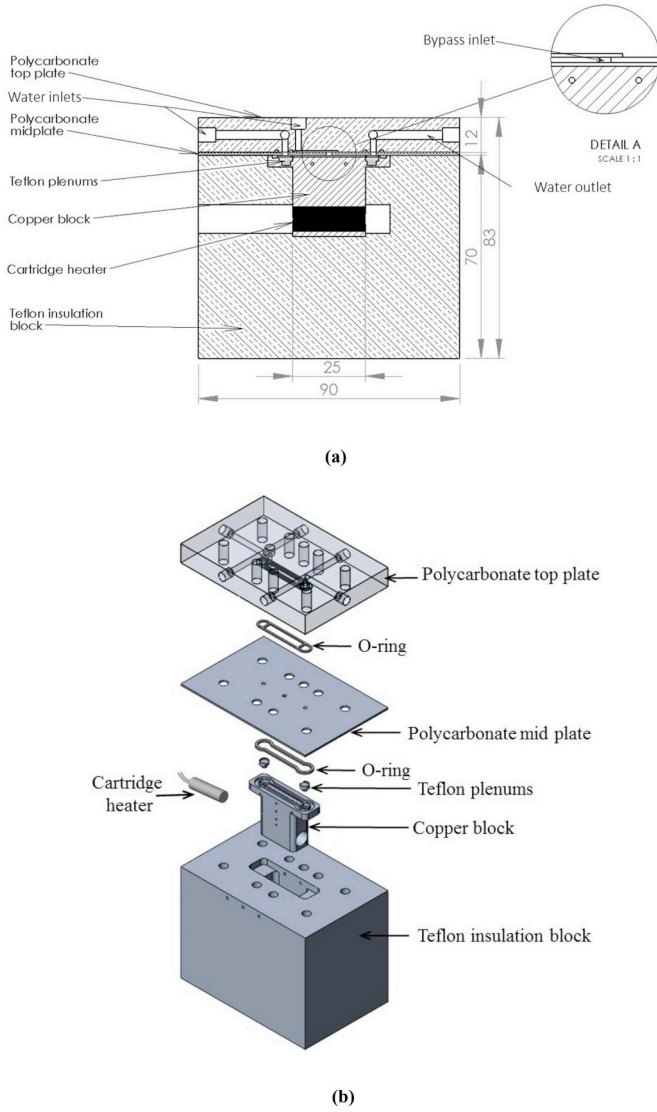
(a)

(b)

Fig. 3. Test section: (a) sectional view and (b) exploded view.

and ($\overline{T}_{tc} - T_{atm}$) for different mass fluxes. Heat loss during the two-phase experiments are obtained by extrapolating this plot as followed in other studies [34–37]. $\overline{T}_{tc}$ is the average of temperatures, $T_{tc,i}$, as shown in Eq. (4). i = 1, 2,.0.5, denotes the individual thermocouples.

$$\overline{T}_{tc} = \frac{1}{n} \sum_{i=1}^{5} T_{tc,i} \tag{4}$$

Heat removed by the micro-channel flow during flow boiling experiments and the corresponding channel heat flux are given by the Eqs. (5) and (6), respectively.

$$Q = Q_{supplied} - Q_{loss} \tag{5}$$

$$q = \frac{Q}{A_s} \tag{6}$$

The heat transfer takes place only through the three sides of primary passage, so the heat transfer surface area is calculated from $A_s = (a + 2b)L$. Wall temperatures are determined using 1-dimensional Fourier's law of heat conduction [37–40] as shown in Eq. (7).

$$T_{w,i} = T_{tc,i} - \frac{q\Delta y}{k} \tag{7}$$

Channel average heat transfer coefficient across the micro-channel

heat sink is obtained from Eq. (8).

$$\overline{h} = \frac{q}{\overline{T}_w - T_{mean}} \tag{8}$$

where $\overline{T}_w$ is the average of wall temperatures at five locations and T_{mean} is the average of channel inlet and outlet temperatures, as shown in Eqs. (9) and (10), respectively.

$$\overline{T}_w = \frac{1}{n} \sum_{i=1}^{5} T_{w,i} \tag{9}$$

$$T_{mean} = \frac{T_i + T_o}{2} \tag{10}$$

Since the proposed design involves the mixing of the flow from the bypass inlet (at the middle of the channel) and the flow through the primary inlet, the channel average heat transfer coefficient is considered for comparison, instead of the two-phase heat transfer coefficient.

Pressure drop across the micro-channel is obtained from Eq. (11).

$$\Delta p_{ch} = \Delta p_{measured} - (\Delta p_{con} - \Delta p_{exp}) \tag{11}$$

where Δp_{ch} is the actual channel pressure drop and $\Delta p_{measured}$ is the pressure drop across micro-channel measured by pressure transmitter. Δp_{con} is the pressure loss due to contraction at the inlet of micro-channel and Δp_{exp} is the pressure recovered due to expansion at the outlet of micro-channel. Pressure loss due to contraction [37–39] can be obtained from Eqs. (12)–(14).

$$\Delta p_{con} = \frac{1}{2} \left[1 - \left(\frac{A_{cs}}{A_p} \right)^2 + K_{con} \right] G^2 \vartheta_f \tag{12}$$

where $K_{con} = 0.0088\alpha^2 - 0.1785\alpha + 1.6027 \tag{13}$

$$\alpha = b/a \tag{14}$$

Pressure recovered due to expansion [37–39] for single-phase and two-phase exit flows are obtained from Eqs. (15) and (16), respectively.

$$\Delta P_{exp,sp} = -1.33 \, G^2 \left(\frac{A_{cs}}{A_p} \right) \left[1 - \left(\frac{A_{cs}}{A_p} \right) \right] \vartheta_{f,o} \tag{15}$$

$$\Delta P_{exp,tp} = G^2 \left(\frac{A_{cs}}{A_p} \right) \left[\left(\frac{A_{cs}}{A_p} \right) - 1 \right] \vartheta_{f,o} (1 - x_e)^2 \left[1 + \frac{C}{X} + \frac{1}{X^2} \right] \tag{16}$$

Pressure at inlet and outlet of the micro-channel is calculated from Eqs. (17) and (18), respectively.

$$p_i = p_{t,i} - \Delta p_{con} \tag{17}$$

$$p_o = p_i - \Delta p_{ch} \tag{18}$$

Exit vapor quality of the fluid is calculated using Eqs. (19) and (20).

$$x_e = \frac{i_e - i_f}{i_g - i_f} \tag{19}$$

where $i_e = i_i + \frac{Q}{\dot{m}} \tag{20}$

The properties of the subcooled liquid at the channel inlet correspond to the channel inlet temperature (97 °C) and the two-phase properties at the channel exit correspond to the channel outlet pressure assuming thermodynamic equilibrium. The exit pressure was in the range 1.02–1.10 bar.

3.1. Repeatability and uncertainties

Experiments were conducted to ensure the repeatability of results with the aged copper micro-channel used in this study. Fig. 6 shows the negligible variation in the channel average heat transfer coefficient
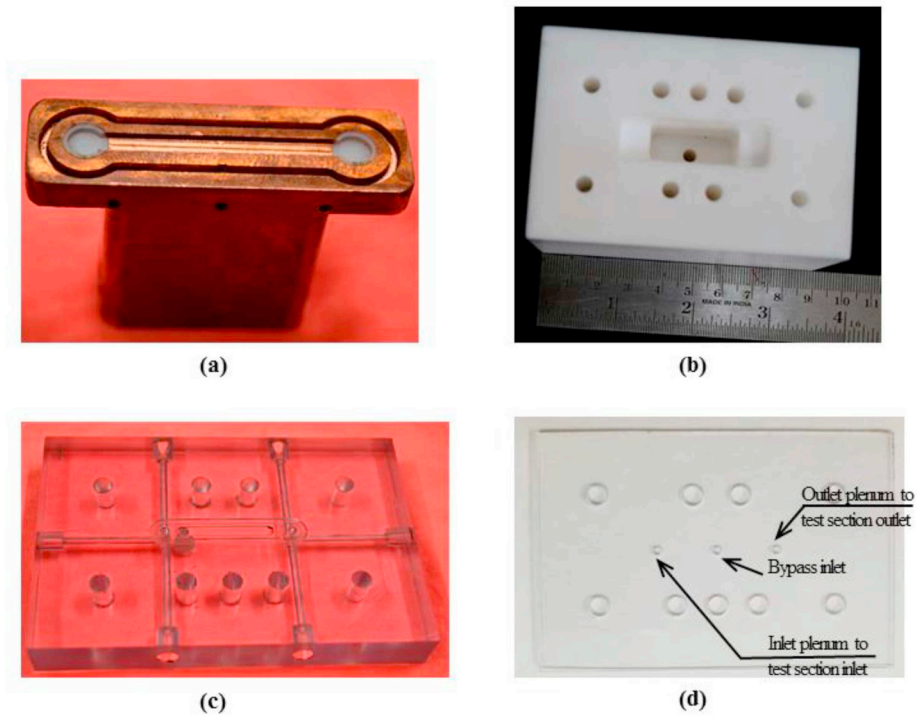
Fig. 4. Components of test section (not to scale): (a) Copper block with primary passage, (b) Teflon insulation block, (c) Polycarbonate top cover with secondary passage, (d) Polycarbonate mid-plate with bypass inlet.
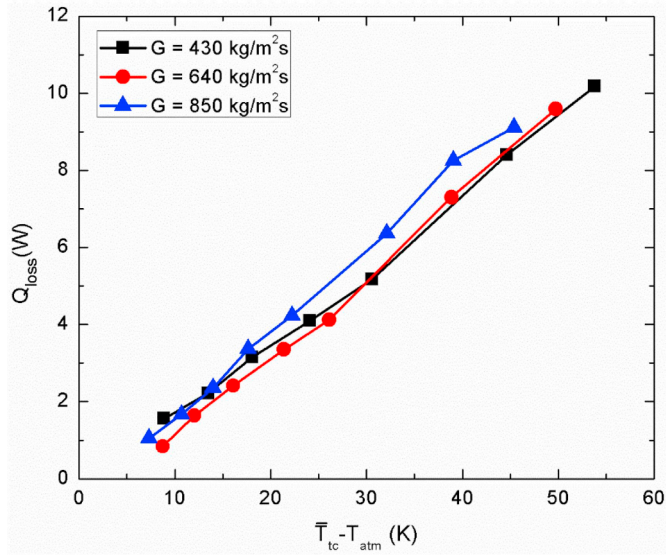

Fig. 5. Heat loss from test section for different flow rates during single phase experiments.

Fig. 6. Repeatability of heat transfer coefficient values from boiling experiments.

obtained in two different experimental runs. Uncertainties due to the systematic errors are estimated from the calibration of the measuring instruments. Uncertainties in derived quantities are obtained by the method suggested by Moffat [41]. When a derived quantity $R(x_1, x_2, \dots x_n)$ is a function of number of fundamental or measured quantities, x_i, and U_{x_i} is the value of uncertainty in x_i, the overall uncertainty in R is given by the Eq. (21).

$$U_R = \pm \sqrt{\sum_{i=1}^{n} \left(\frac{\partial R}{\partial x_i} U_{x_i} \right)^2} \tag{21}$$

The uncertainties obtained for measured and derived quantities are listed in Table 1. Uncertainties in the channel dimensions mentioned in
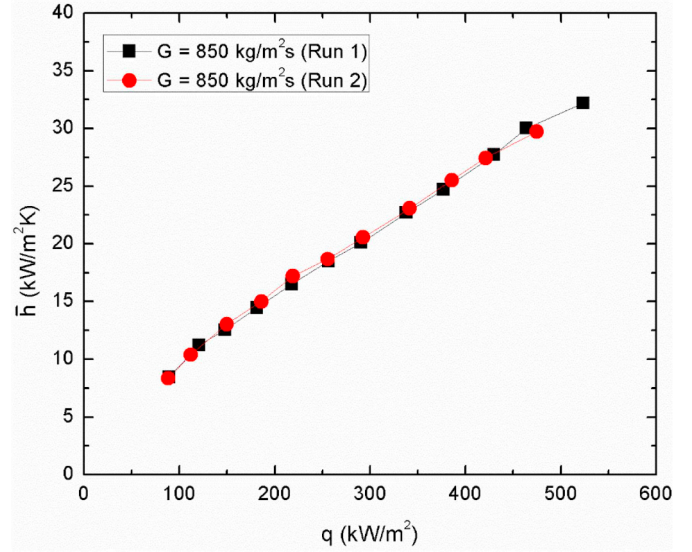
Table 1 are the standard deviations of the measured values at different points of the channel.

4. Results and discussion

4.1. Validation with single phase experiments

Experimental setup, test section and methodology were validated with single phase experiments before conducting flow boiling experiments. The frictional pressure drop data obtained for the conventional micro-channel used in this study is compared with the Shah correlation [42] and Muzychka correlation [43]. Both the correlations were recommended for laminar developing flow in non-circular ducts. Fig. 7

Table 1
Uncertainties in measured and derived quantities.

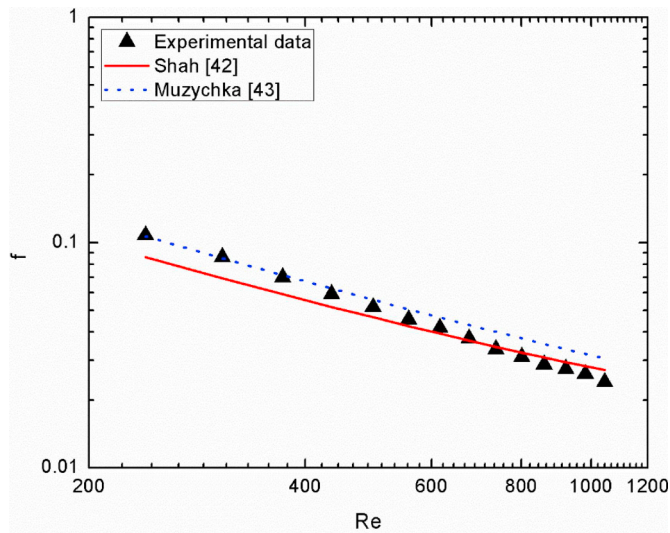| Quantity	Uncertainty
Channel width	± 0.004 mm
Channel depth	± 0.008 mm
Channel length	± 0.05 mm
Power supply, voltage	± 1 V
Power supply, current	± 0.01 A
Thermocouple	± 0.4 K
Pressure transmitter	± 0.33 kPa
Flow meter	± 0.2 ml/min
Heat flux	± 1.89%
Mass flux	± 1.48%
Single-phase friction factor	± 14.4%
Single-phase Nusselt number	± 14.5%
Two-phase heat transfer coefficient	± 12.6%

Fig. 7. Comparison of experimental friction factor data with predicted values from correlations.
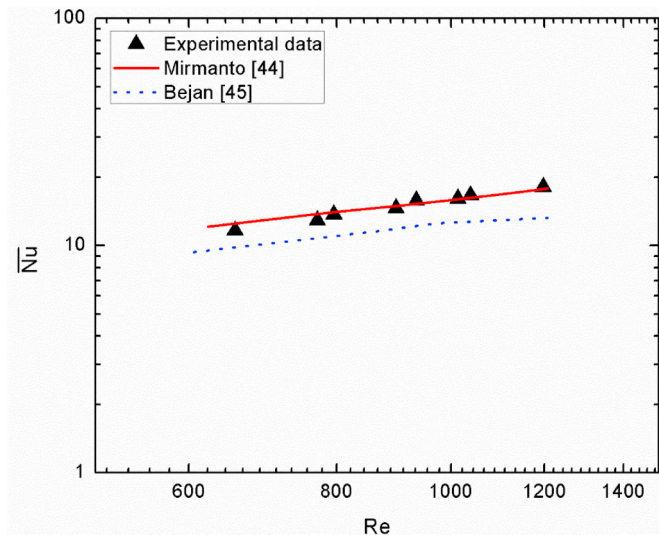

Fig. 8. Comparison of experimental Nusselt number with predicted values from correlations.

illustrates that the experimental friction factor matches closely the values predicted by both the correlations. The deviation (mean absolute error) between the data predicted by the Shah correlation [42] and the present experimental data is 12%. Fig. 8 presents the comparison of
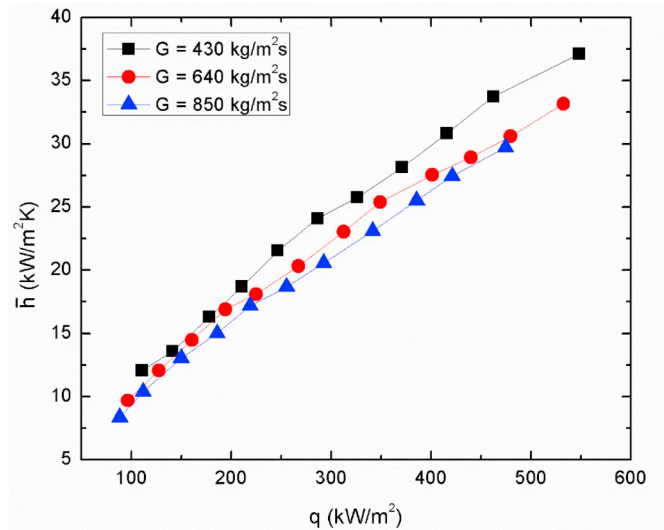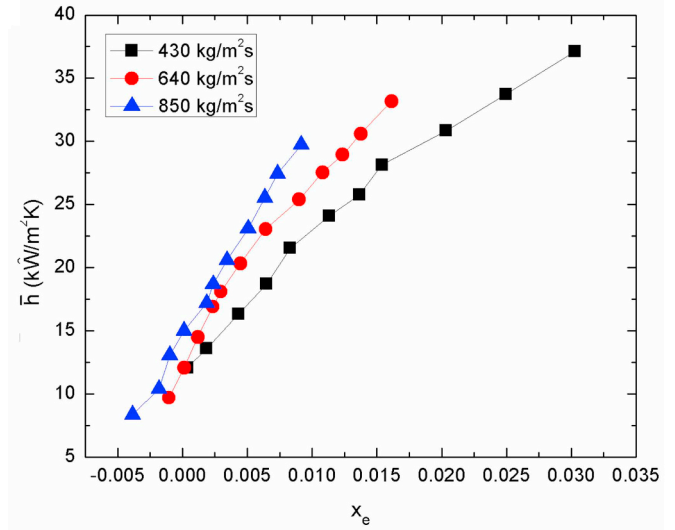
Fig. 9. Variation of two-phase heat transfer coefficients with (a) heat flux and (b) exit vapor quality.

average single phase experimental Nusselt number with two correlations. The deviations (mean absolute error) between the present experimental data and the data predicted by the Mirmanto correlation [44] and Bejan correlation [45] are 5% and 21%, respectively. Mirmanto correlation [44] was developed from non-circular channel data unlike Bejan correlation [45].

4.2. Flow boiling results without bypass flow

Experiments were conducted initially without bypassing the flow for three different mass fluxes. Variation of channel heat transfer coefficient with heat flux and exit quality for different mass fluxes is shown in Fig. 9. From Fig. 9(a), it can be seen that the heat transfer coefficient strongly depends on the heat flux. As the heat flux increases from 87 kW/m^2 to 548 kW/m^2, the heat transfer coefficient increases from approximately 10 kW/m^{2}K to around 30 kW/m^{2}K, suggesting the nucleate boiling dominant mechanism. The heat transfer coefficient decreases by about 20% as the mass flux increases from 430 kg/m^2 s to 850 kg/m^2 s. The decrease can be attributed to the possible suppression
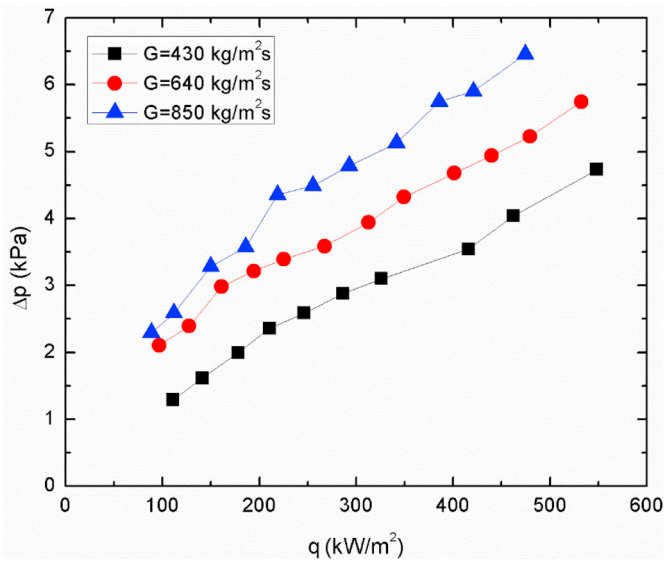
**Fig. 10.** Pressure drop variation with heat flux.

of nucleation caused by higher mass fluxes. For the same exit quality, higher mass flux results in higher average heat transfer coefficient. This is because the heat flux will also be higher for higher mass flux for the same exit quality. The channel pressure drop variation with the heat flux is shown in Fig. 10. With the increase in heat flux, the pressure drop increases due to the increased acceleration. The pressure drop also increases with the mass flux due to the increase in frictional pressure drop.

### 4.3. Effect of bypass inlet on two-phase heat transfer

With the proposed bypass flow configuration, the flow rate through the primary passage is only a fraction of the total flow rate. The remaining fraction flows through the secondary passage and enters the channel via the bypass inlet located at the middle of the channel. The bypass ratio was varied to study its influence on the channel heat transfer performance. Fig. 11 shows the influence of bypass ratio on the channel average heat transfer coefficient for different mass fluxes. Fig. 11(a) shows the comparison between the heat transfer coefficient without and with 50% bypass for a total mass flux of 430 kg/m^2 s. A very small increase in the heat transfer coefficient (which lies within the uncertainty limit) can be noticed for the bypass case for the exit
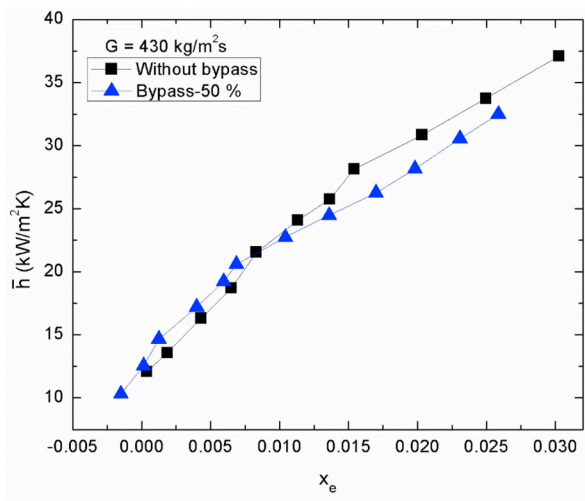
(a)
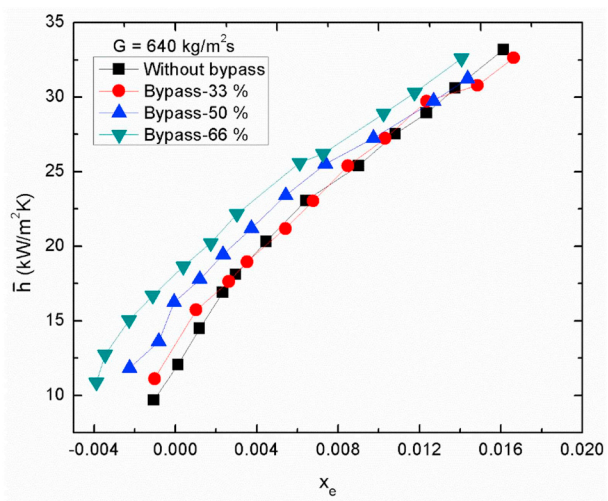
(b)
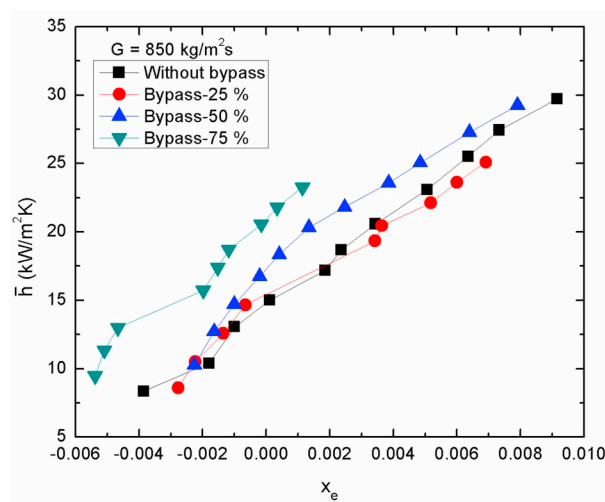
(c)

Fig. 11. Variation of two-phase heat transfer coefficients with exit vapor quality for (a) G = 430 kg/m^2 s, (b) G = 640 kg/m^2 s and (c) G = 850 kg/m^2 s.
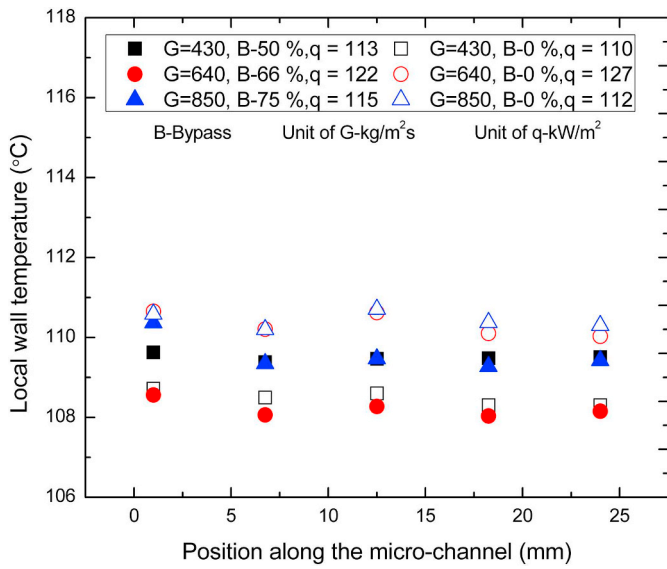
Fig. 12. Comparison of local wall temperatures without bypass and with maximum bypass.

qualities around zero. At higher exit qualities, there is deterioration in the heat transfer coefficient for the bypass case. Fig. 11(b) presents the heat transfer performance for a total mass flux of 640 kg/m² s and for bypass percentages of 0, 33, 50 and 66. A large increase in the heat transfer coefficient with the decrease in the negative exit thermodynamic quality suggests the occurrence of sub-cooled boiling in the channel. With the increase in the bypass percentage from 0 to 66%, the heat transfer coefficient increases significantly with the maximum increase varying from around 30% to 60% for the exit qualities close to zero (which indicate subcooled boiling in the channel). However the extent of the increase in the heat transfer coefficient with the increase in the bypass ratio decreases as the exit quality increases. The bypass effect is almost negligible close to the maximum exit qualities considered in the present study. Similar overall trends can be noticed for a total mass flux of 850 kg/m² s and for bypass percentages of 0, 25, 50 and 75, as shown in Fig. 11(c). But, for this mass flux case, only 75% bypass case shows a significant increase in the heat transfer coefficient and the other bypass ratios show almost no change in the heat transfer
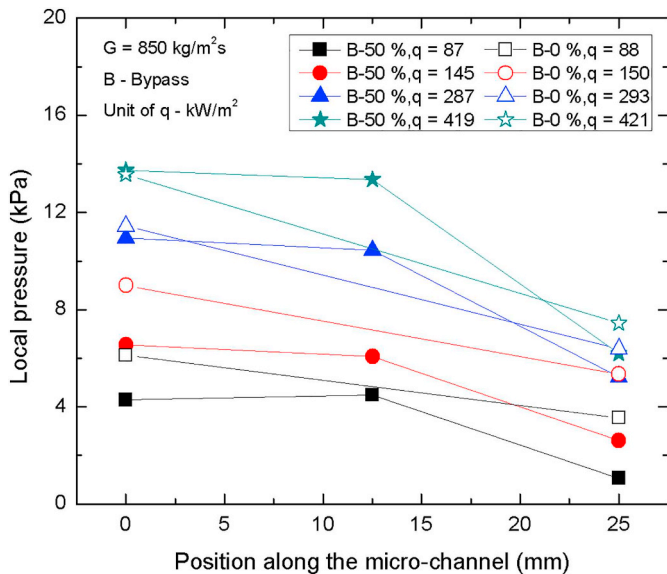

Fig. 13. Channel gauge pressure at different locations for different heat fluxes for G = 850 kg/m² s, without bypass and with 50% bypass.
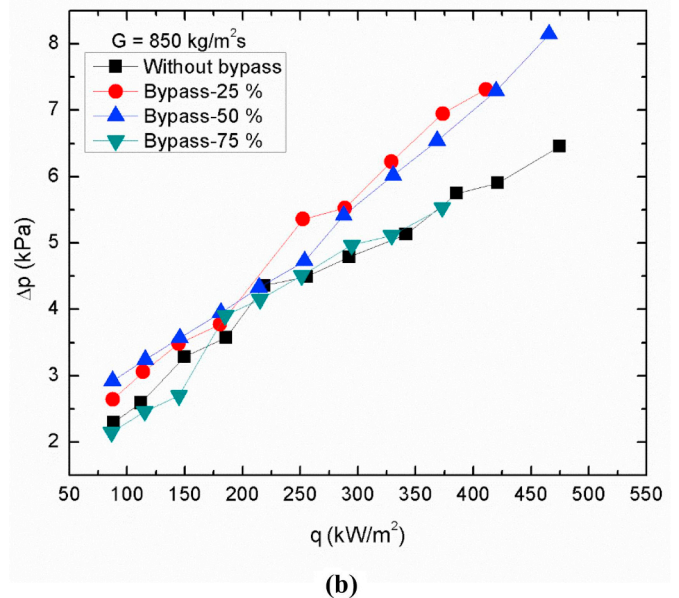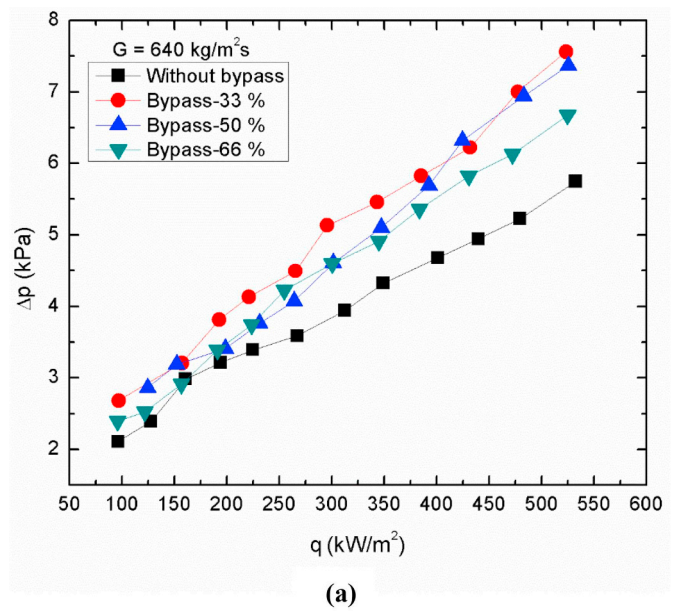

(a)

(b)

Fig. 14. Comparison of pressure drop with and without bypass inlet for (a) G = 640 kg/m² s and (b) G = 850 kg/m² s.

coefficient for the negative exit qualities. However for the exit qualities greater than zero but close to zero, there is an increase in the heat transfer coefficient with the increase in the bypass ratio. At higher exit qualities, 25% bypass case shows a slight decrease and 50% bypass case shows a slight increase in the heat transfer coefficient compared to without bypass case.

Fig. 12 shows the wall temperatures along the channel for the heat flux around 110 kW/m² and three mass fluxes without bypass and with maximum bypass. The wall temperatures decrease due to the bypass for the chosen heat flux that results in nearly subcooled boiling. The temperature variation along the channel is not significant due to the substrate (copper) conduction effect.

The results can be explained based on the influence of the thermofluidics of the proposed bypass scheme on the boiling performance. There will be an effect of mass flux on the incipience of nucleate boiling over the first half of the channel length. The impingement of slightly sub-cooled liquid from the bypass inlet, its consequent mixing with the two-phase flow from the primary passage and the increased mass flux

influence the hydrodynamics and two-phase heat transfer over the second half of the channel length. With the increase in bypass ratio, the mass flux over the first half of the channel length decreases. The decrease in mass flux reduces the suppression of nucleation caused by the thinning of thermal boundary layer. Therefore the boiling incipience is enhanced by the increase in the bypass ratio and hence results in higher heat transfer coefficient. This seems to be the major influencing factor for higher mass fluxes (that tend to suppress the nucleation without bypass) for the subcooled boiling or the exit qualities around zero. Higher mass fluxes also result in the prevalence of subcooled boiling. For the qualities sufficiently greater than zero, the effect is either insignificant or even negative. This is perhaps due to the detriment in the heat transfer coefficient caused by the injection and the impingement of subcooled liquid from the bypass inlet that possibly condenses and or breaks the vapor bubbles. Further, the increased mass flux over the latter half of the channel length can also hinder the boiling. Thus it can be inferred that the proposed bypass scheme has a positive effect on the heat transfer coefficient mainly for subcooled boiling.

4.4. Effect of bypass inlet on pressure drop

Fig. 13 depicts the gauge pressure at inlet and outlet and also at the middle for the bypass cases. The pressure reduction for the bypass case is large after the bypass inlet due to the increased mass flux. The pressure increase due to the bypass is around 15 to 30% for 640 kg/m² s and 850 kg/m² s as shown in Figs. 14(a) and 14(b), respectively. One would expect a lower pressure drop for the bypass case due to the reduction in mass flux through the primary passage, but the observed pressure drop is higher for most of the bypass cases. This can be attributed to the increase in pressure losses due to the impingement effect at the bypass inlet. The increase in pressure drop is relatively small for the maximum bypass cases possibly due to the higher reduction in pressure drop over the first half of the channel length.

5. Conclusions

An experimental investigation was carried out to study the effect of bypass inlet on flow boiling of water in an aged copper mini/microchannel. The major conclusions that can be drawn from the study are as follows.

1. Results indicate that the proposed bypass scheme enhances the heat transfer coefficient mainly for the boiling close to subcooled condition. The enhancement increases with the bypass ratio. The improvement was observed for higher mass fluxes. For the mass flux of 430 kg/m² s, the effect was almost negligible. For the case of 640 kg/m² s mass flux, the increase in the bypass percentage from 0 to 66% increases the heat transfer coefficient by around 30% to 60% for the exit qualities close to zero. The enhancement decreases as the exit quality increases. The results with 850 kg/m² s are also almost similar.

2. The enhancement in heat transfer performance is attributed to the promotion of boiling incipience by the reduced mass fluxes through the primary passage. However, the factors such as the injection and the impingement of subcooled liquid from the bypass inlet that probably condenses and or breaks the vapor bubbles and the increased mass flux over the second half of the channel seem to reduce the enhancement at higher exit qualities.

3. There is a 15 to 30% increase in total pressure drop due to the bypass for the mass fluxes considered in the study. The increase is perhaps due to the impingement effect at the bypass inlet. However, for the maximum bypass cases the increase in total pressure drop is relatively small due to the higher reduction in pressure drop caused by the decreased mass flux over the first half of the channel length.

4. It may be noted that the present results are for the bypass inlet located at the middle of a channel of 25 mm length. The results may be influenced by the location of bypass inlet and also the length of the channel, which need to be investigated. Also the factors such as the injection and the impingement of subcooled liquid from the bypass inlet that perhaps condenses and or breaks the vapor bubbles resulting in the deterioration of heat transfer coefficient may in fact increase the critical heat flux. This can be a scope for the future study, considering a possibly enhanced boiling caused by a reduced mass flux over a portion of the channel and a delayed critical heat flux (dryout or departure from nucleate boiling) caused by the thermo-fluidics associated with the bypass inlet configuration.

6. Nomenclature

a	width of micro-channel, m
A	area, m²
b	height of micro-channel, m
c_p	specific heat, J/kgK
C	constant
D_h	channel hydraulic diameter, $D_h = 2ab/(a + b)$, m
f	Fanning friction factor
G	mass flux, kg/m²s
h	heat transfer coefficient, W/m²K
i	enthalpy, J/kg
I	current, I
k	thermal conductivity, W/mK
K	(constant)
L	length of micro-channel, m
$\dot{m}$	mass flow rate, kg/s
Nu	Nusselt number
p	pressure, Pa
Δp	pressure drop, Pa
q	heat flux, W/m²
Q	heat rate, W
Re	Reynolds number
T	temperature, K
V	voltage, V
x	thermodynamic equilibrium quality
X	Martinelli parameter
Δy	distance, m

6.1. Greek symbols

α	channel aspect ratio = b/a
ϑ	specific volume, m³/kg

6.2. Subscripts

atm	(atmosphere)
ch	(channel)
con	(contraction)
cs	(cross-section)
e	(exit)
eff	(effective)
exp	(expansion)
f	(fluid)
g	(gaseous)
i	(inlet)
o	(outlet)
p	(plenum)
s	(surface)
sat	(saturated)
t	(transmitter)
tc	(thermocouple)
w	(wall)

References

[1] D.B. Tuckerman, R.F.W. Pease, High-performance heat sinking for VLSI High-Performance Heat Sinking for VLSI, IEEE Electron Device Lett. 2 (5) (1981) 126–129, https://doi.org/10.1109/EDL.1981.25367.

[2] S.G. Kandlikar, S. Colin, Y. Peles, S. Garimella, R.F. Pease, J.J. Brandner, D.B. Tuckerman, Heat transfer in microchannels—2012 status and research needs, J. Heat Transf. 135 (2013) 91001, , https://doi.org/10.1115/1.4024354.

[3] M.P. David, A. Marconnet, K.E. Goodson, Hydrodynamic and thermal performance of a vapor-venting microchannel copper heat exchanger, ICNMM2008–62269. (2008) 1–8.

[4] A. Koşar, C.J. Kuo, Y. Peles, Boiling heat transfer in rectangular microchannels with reentrant cavities, Int. J. Heat Mass Transf. 48 (2005) 4867–4886, https://doi.org/10.1016/j.ijheatmasstransfer.2005.06.003.

[5] A. Koşar, C.-J. Kuo, Y. Peles, Suppression of boiling flow oscillations in parallel microchannels by inlet restrictors, J. Heat Transf. 128 (2006) 251, https://doi.org/10.1115/1.2150837.

[6] S.G. Kandlikar, W.K. Kuan, D.A. Willistein, J. Borrelli, Stabilization of flow boiling in microchannels using pressure drop elements and fabricated nucleation sites, J. Heat Transf. 128 (2006) 389, https://doi.org/10.1115/1.2165208.

[7] A. Mukherjee, S.G. Kandlikar, The effect of inlet constriction on bubble growth during flow boiling in microchannels, Int. J. Heat Mass Transf. 52 (2009) 5204–5212, https://doi.org/10.1016/j.ijheatmasstransfer.2009.04.025.

[8] J.Y. Lee, M.H. Kim, M. Kaviany, S.Y. Son, Bubble nucleation in microchannel flow boiling using single artificial cavity, Int. J. Heat Mass Transf. 54 (2011) 5139–5148, https://doi.org/10.1016/j.ijheatmasstransfer.2011.08.042.

[9] S.G. Kandlikar, History, advances, and challenges in liquid flow and flow boiling heat transfer in microchannels: a critical review, J. Heat Transf. 134 (2012) 034001, , https://doi.org/10.1115/1.4005126.

[10] Z. Wu, B. Sundén, On further enhancement of single-phase and flow boiling heat transfer in micro/minichannels, Renew. Sust. Energ. Rev. 40 (2014) 11–27, https://doi.org/10.1016/j.rser.2014.07.171.

[11] N.A.C. Sidik, M.N.A.W. Muhamad, W.M.A.A. Japar, Z.A. Rasid, An overview of passive techniques for heat transfer augmentation in microchannel heat sink, Int. Commun. Heat Mass Transf. 88 (2017) 74–83, https://doi.org/10.1016/j.icheatmasstransfer.2017.08.009.

[12] G. Narendran, N. Gnanasekaran, D.A. Perumal, A review on recent advances in microchannel heat sink configurations, Recent Patents Mech. Eng. 11 (2018) 190–215, https://doi.org/10.1016/j.molcel.2010.08.005.

[13] S. Lu, K. Vafai, A comparative analysis of innovative microchannel heat sinks for electronic cooling, Int. Commun. Heat Mass Transf. 76 (2016) 271–284, https://doi.org/10.1016/j.icheatmasstransfer.2016.04.024.

[14] A. Dewan, P. Srivastava, A review of heat transfer enhancement through flow disruption in a microchannel, J. Therm. Sci. 24 (2015) 203–214, https://doi.org/10.1007/s11630-015-0775-1.

[15] I.A. Ghani, N.A.C. Sidik, N. Kamaruzaman, Hydrothermal performance of microchannel heat sink: the effect of channel design, Int. J. Heat Mass Transf. 107 (2017) 21–44, https://doi.org/10.1016/j.ijheatmasstransfer.2016.11.031.

[16] V. Khanikar, I. Mudawar, T. Fisher, Flow boiling in a Micro-Channel coated with carbon nanotubes, IEEE Trans. Componenets Packag. Technol. 32 (2009), https://doi.org/10.1109/TCAPT.2009.2015232.

[17] N. Singh, V. Sathyamurthy, W. Peterson, J. Arendt, D. Banerjee, Flow boiling enhancement on a horizontal heater using carbon nanotube coatings, Int. J. Heat Fluid Flow 31 (2010) 201–207, https://doi.org/10.1016/j.ijheatfluidflow.2009.11.002.

[18] S. Vafaei, D. Wen, Flow boiling heat transfer of alumina nanofluids in single microchannels and the roles of nanoparticles, J. Nanopart. Res. 13 (2011) 1063–1073, https://doi.org/10.1007/s11051-010-0095-z.

[19] L. Xu, J. Xu, Nanofluid stabilizes and enhances convective boiling heat transfer in a single microchannel, Int. J. Heat Mass Transf. 55 (2012) 5673–5686, https://doi.org/10.1016/j.ijheatmasstransfer.2012.05.063.

[20] K. Balasubramanian, P.S. Lee, L.W. Jin, S.K. Chou, C.J. Teo, S. Gao, Experimental investigations of flow boiling heat transfer and pressure drop in straight and expanding microchannels - a comparative study, Int. J. Therm. Sci. 50 (2011) 2413–2421, https://doi.org/10.1016/j.ijthermalsci.2011.07.007.

[21] C.T. Lu, C. Pan, Convective boiling in a parallel microchannel heat sink with a diverging cross section and artificial nucleation sites, Exp. Thermal Fluid Sci. 35 (2011) 810–815, https://doi.org/10.1016/j.expthermflusci.2010.08.018.

[22] A. Kalani, S.G. Kandlikar, Flow patterns and heat transfer mechanisms during flow boiling over open microchannels in tapered manifold (OMM), Int. J. Heat Mass Transf. 89 (2015) 494–504, https://doi.org/10.1016/j.ijheatmasstransfer.2015.05.070.

[23] M. Law, P.S. Lee, K. Balasubramanian, Experimental investigation of flow boiling heat transfer in novel oblique-finned microchannels, Int. J. Heat Mass Transf. 76 (2014) 419–431, https://doi.org/10.1016/j.ijheatmasstransfer.2014.04.045.

[24] M. Law, P.S. Lee, A comparative study of experimental flow boiling heat transfer and pressure characteristics in straight- and oblique-finned microchannels, Int. J. Heat Mass Transf. 85 (2015) 797–810, https://doi.org/10.1016/j.ijheatmasstransfer.2015.01.137.

[25] Y.K. Prajapati, M. Pathak, M.K. Khan, Bubble dynamics and flow boiling characteristics in three different microchannel configurations, Int. J. Therm. Sci. 112 (2017) 371–382, https://doi.org/10.1016/j.ijthermalsci.2016.10.021.

[26] K. Balasubramanian, P.S. Lee, C.J. Teo, S.K. Chou, Flow boiling heat transfer and pressure drop in stepped fin microchannels, Int. J. Heat Mass Transf. 67 (2013) 234–252, https://doi.org/10.1016/j.ijheatmasstransfer.2013.08.023.

[27] M.K. Sung, I. Mudawar, Single-phase and two-phase cooling using hybrid microchannel/slot-jet module, Int. J. Heat Mass Transf. 51 (2008) 3825–3839, https://doi.org/10.1016/j.ijheatmasstransfer.2007.12.015.

[28] I. Mudawar, Recent advances in high-flux, two-phase thermal management, J. Therm. Sci. Eng. Appl. 5 (2013) 021012, , https://doi.org/10.1115/1.4023599.

[29] M.K. Sung, I. Mudawar, Single-phase and two-phase heat transfer characteristics of low temperature hybrid micro-channel/micro-jet impingement cooling module, Int. J. Heat Mass Transf. 51 (2008) 3882–3895, https://doi.org/10.1016/j.ijheatmasstransfer.2007.12.016.

[30] M.K. Sung, I. Mudawar, Single-phase and two-phase hybrid cooling schemes for high-heat-flux thermal management of defense electronics, 2008 11th IEEE Intersoc. Conf. Therm. Thermomechanical Phenom. Electron. Syst. I-THERM. 131 (2008) 121–131, https://doi.org/10.1109/ITHERM.2008.4544262.

[31] J. Barrau, D. Chemisana, J. Rosell, L. Tadrist, M. Ibañez, An experimental study of a new hybrid jet impingement/micro-channel cooling scheme, Appl. Therm. Eng. 30 (2010) 2058–2066, https://doi.org/10.1016/j.applthermaleng.2011.10.001.

[32] J. Barrau, M. Omri, D. Chemisana, J. Rosell, M. Ibañez, L. Tadrist, Numerical study of a hybrid jet impingement/micro-channel cooling scheme, Appl. Therm. Eng. 33–34 (2011) 237–245, https://doi.org/10.1016/j.applthermaleng.2011.10.001.

[33] J. Barrau, A. Perona, A. Dollet, J. Rosell, Outdoor test of a hybrid jet impingement/micro-channel cooling device for densely packed concentrated photovoltaic cells, Sol. Energy 107 (2014) 113–121, https://doi.org/10.1016/j.solener.2014.05.040.

[34] M. Mirmanto, International journal of heat and mass transfer heat transfer coefficient calculated using a linear pressure gradient assumption and measurement for flow boiling in microchannels, Int. J. Heat Mass Transf. 79 (2014) 269–278, https://doi.org/10.1016/j.ijheatmasstransfer.2014.08.022.

[35] E.A. Pike-Wilson, T.G. Karayiannis, Flow boiling of R245fa in 1.1mm diameter stainless steel, brass and copper tubes, Exp. Thermal Fluid Sci. 59 (2014) 166–183, https://doi.org/10.1016/j.expthermflusci.2014.02.024.

[36] M.M. Mahmoud, T.G. Karayiannis, D.B.R. Kenning, Surface effects in flow boiling of R134a in microtubes, Int. J. Heat Mass Transf. 54 (2011) 3334–3346, https://doi.org/10.1016/j.ijheatmasstransfer.2011.03.052.

[37] P. Jayaramu, S. Gedupudi, S.K. Das, Influence of heating surface characteristics on flow boiling in a copper microchannel: experimental investigation and assessment of correlations, Int. J. Heat Mass Transf. 128 (2019) 290–318, https://doi.org/10.1016/j.ijheatmasstransfer.2018.08.075.

[38] B.J. Jones, S.V. Garimella, Surface roughness effects on flow boiling in microchannels, J. Therm. Sci. Eng. Appl. 1 (2010) 041007, , https://doi.org/10.1115/1.4001804.

[39] P.S. Lee, S.V. Garimella, Saturated flow boiling heat transfer and pressure drop in silicon microchannel arrays, Int. J. Heat Mass Transf. 51 (2008) 789–806, https://doi.org/10.1016/j.ijheatmasstransfer.2007.04.019.

[40] M.E. Steinke, S.G. Kandlikar, An experimental investigation of flow boiling characteristics of water in parallel microchannels, J. Heat Transf. 126 (2004) 518, https://doi.org/10.1115/1.1778187.

[41] R.J. Moffat, Describing the uncertainties in experimental results, Exp. Thermal Fluid Sci. 1 (1988) 3–17, https://doi.org/10.1016/0894-1777(88)90043-X.

[42] R.K. Shah, A correlation for laminar hydrodynamic entry length solutions for circular and noncircular ducts, J. Fluids Eng. 100 (1978) 177–179.

[43] Y.S. Muzychka, M.M. Yovanovich, Pressure drop in laminar developing flow in noncircular ducts: a scaling and modeling approach, J. Fluids Eng. 131 (2009) 111105, , https://doi.org/10.1115/1.4000377.

[44] Mirmanto, Single-Phase Flow and Flow Boiling of Water in Horizontal Rectangular Microchannels, Ph.D Diss. Brunnel Univ., UK, 2013.

[45] A. Bejan, Convection Heat Transfer, Fourth edition, Wiley, India, 2013, https://doi.org/10.1002/9781118671627.